Heteroatom Chemistry
Volume 2, Number 1, 1991

Reactivity in Molecular Crystals: Radical Formation in Chiral Phosphorus Compounds

Olav M. Aagaard,* René A. J. Janssen, Bas F. M. de Waal, and Henk M. Buck

Contribution from the Department of Organic Chemistry, Eindhoven University of Technology, P.O. Box 513, 5600 MB Eindhoven, The Netherlands

Received 26 June 1990.

ABSTRACT

Molecular mechanics calculations, using the AMBER program (version 3.0), are presented on the radiogenic electron-capture radical formation in the crystalline chiral organophosphorus compounds (2R,4S,5R) and (2S,4S,5R) 2-chloro-3,4-dimethyl-5-phenylphospholidine 2-sulfide (respectively **1** *and* **2**). *Geometry optimization of the corresponding radical anion structures and their respective crystal surroundings reveals an increase of the Van der Waals interactions, which is significantly larger in compound* **2** *than in* **1**. *This is in good agreement with previous single-crystal ESR experiments and molecular interactions calculations without geometry optimization* [1].

INTRODUCTION

Recently we reported on the differences encountered in the radical formation after X irradiation in the chiral organophosphorus compounds (2R,4S,5R) and (2S,4S,5R) 2-chloro-3,4-dimethyl-5-phenylphospholidine 2-sulfide (respectively **1** and **2**) [1]. Compound **1** rendered a phosphoranyl type radical (**1a**) via an electron-capture process when in a crystalline state and when dissolved in a frozen host matrix (diethyl ether or 2-methyl-tetrahydrofuran, see Figure 1). The characterization of the phosphoranyl radical anion **1a** in crystalline **1** was performed by single-crystal ESR methods and its structure was assigned to a three electron bond between phosphorus and chlorine in which the odd electron resides in the antibonding σ^* orbital (so called P∴Cl σ^*). In contrast the corresponding radical anion **2a** of the diastereoisomeric form **2** is absent after X irradiation of a crystalline sample and can only be formed in a frozen host matrix.

The explanation of this phenomenon was found in the "topochemical control" [2] (i.e. the expression of the intrinsic reactivity of a precursor molecule is favored or disfavored by its surroundings) of the electron-capture reaction by the crystal environment of the radical precursors **1** and **2**, permitting the formation of **1a** in **1** and inhibiting **2a** in **2**. Formation of **1a** and **2a** in equal amounts in a host matrix corroborates the importance of intermolecular effects and precludes the possibility that the two precursors **1** and **2** possess a different intrinsic reactivity towards electron capture.

The formation of a P∴Cl σ^* radical must be accompanied by an elongation of the P—Cl bond in order to form a stable intermediate. In a tightly packed crystal this elongation will result in an increase of the Van der Waals interactions. We examined the topochemical control of the radiogenic P∴Cl σ^* bond formation by calculating the change of the Van der Waals energy as a function of the length and orientation of the P∴Cl σ^* bond in a crystal environment. The calculations showed that the increase of the Van der Waals energy was higher in **2** than in **1**, which is in good agreement with the single-crystal ESR experiments [1].

In this paper we extend our modelling studies by allowing both the radical and its crystal surroundings to adjust their geometries to the P∴Cl σ^* radical formation. For this purpose we used the AMBER molecular mechanics program [3] to min-

*To whom correspondence should be addressed.

1042-7163/91/$3.50 + .25

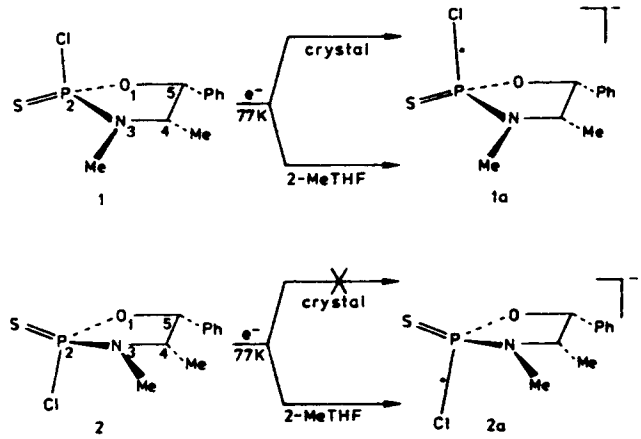

FIGURE 1 Radical formation in compounds **1** and **2** after exposure to X rays in crystalline state and being dissolved in a frozen 2-methyl-tetrahydrofuran host matrix.

imize the total energy and to optimize the geometries. The calculations show a good accord with the single-crystal experiments in which Van der Waals interactions are indeed larger in **2** than in **1**.

METHODS

The initial structures were obtained from the crystallographic data of Bartczak et al. [4]. The data of the C_7 hydrogens of molecule **2** were adjusted to obtain a pure tetragonal carbon atom. A unit cell was constructed applying the symmetry rules of the $P2_12_12_1$ space group (No. 19, x,y,z; $\frac{1}{2} - x, -y, \frac{1}{2} + z$; $\frac{1}{2} + x, \frac{1}{2} - y, -z$; $-x, \frac{1}{2} + y, \frac{1}{2} - z$). This unit cell was then copied and translated into a total of 27 unit cells in the shape of a 3 × 3 × 3 cube. The reacting molecule is contained in the central cell and is surrounded by 107 other molecules. Net atomic charges were calculated with MNDO using the AMPAC program [5] and are given in Figure 2. The standard AMBER potential function was used covering bond stretching, bond bending, torsional, Van der Waals, and electrostatic interactions [6]. Harmonic force constants were taken from the standard AMBER all-atom force field [7], and equilibrium

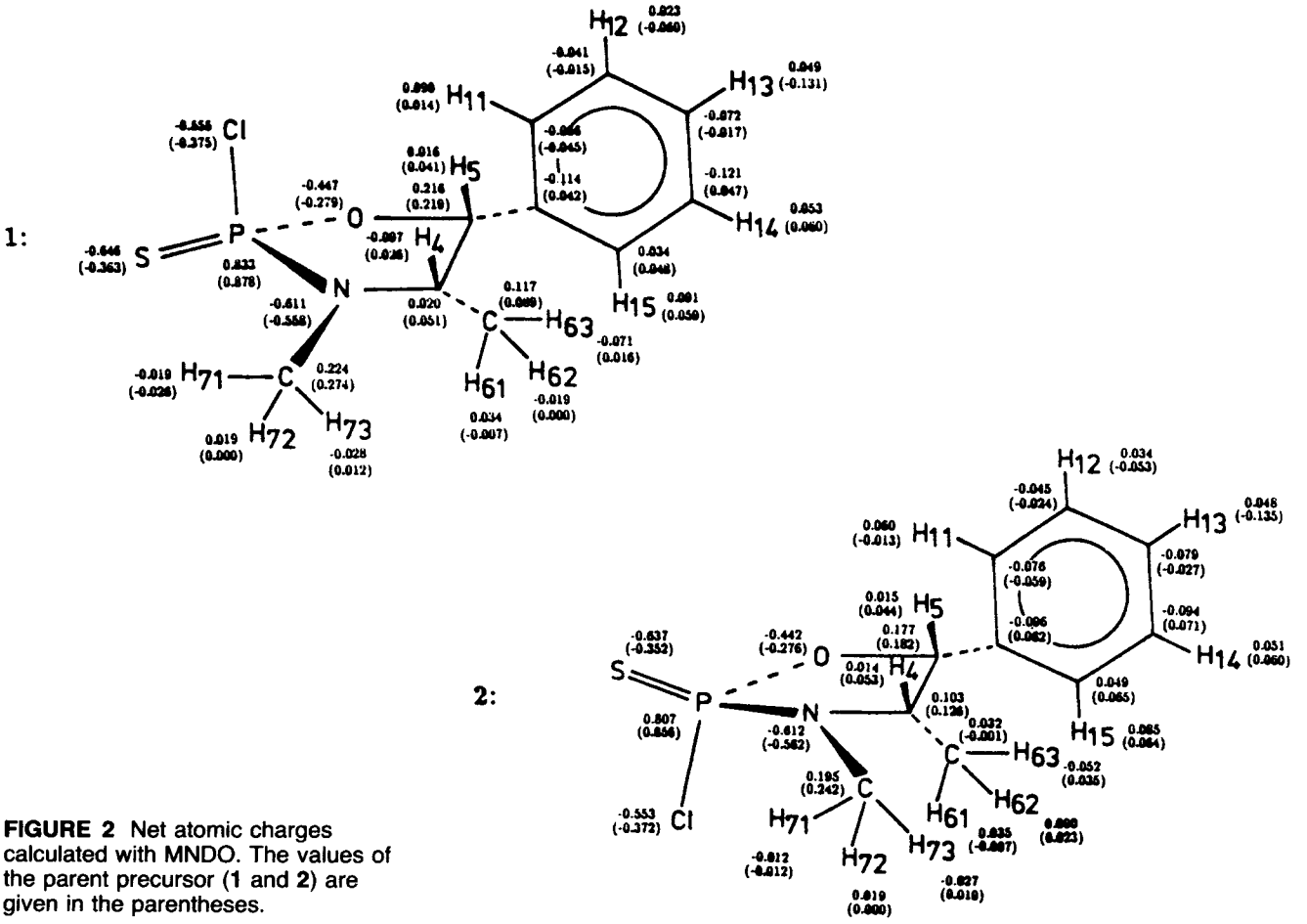

FIGURE 2 Net atomic charges calculated with MNDO. The values of the parent precursor (**1** and **2**) are given in the parentheses.

bond lengths and bond angles were adjusted to match the crystal values.

We obtained the harmonic force constants for the nonstandard bond lengths from the Lange's Handbook of Chemistry [8]; they were scaled according to values present in the standard force field (scaling factor: 1.61 based on the P—O bond). The harmonic force constants for nonstandard bond angles were set to 50 kcal/mol, rad^2. A threefold torsion potential was assumed for the X–N2–P–X dihedral ($V_{3/2}$ = 0.75 kcal/mol, γ = 0). The Van der Waals parameters were taken from our earlier calculations [1, 9]. Based on the net one bonding electron residing in the P⋯Cl σ^* bond we chose the harmonic force constant for the bond length to be half the harmonic force constant of a normal P—Cl bond. The equilibrium bond length of the P⋯Cl σ^* bond was set to 2.80 Å analogous to a calculated increase of 40% in the bond length in the P⋯P σ^* type radical [10]. The SPCl equilibrium bond angle in the radical was chosen as 120°, based on the possible admixture of a trigonal-bipyramidal configuration with the sulfur and chlorine atoms in axial positions and the unpaired electron in an equatorial position (TBP-e) [11].

All molecules within an 8 Å vicinity of the reacting P—Cl bond were allowed to optimize their geometry (15 molecules in both **1** and **2**), and the rest were frozen (92 molecules by using the partial belly optimization option). The dielectric constant ϵ was set to 2.5. A combination of 250 steps steepest descent and subsequent conjugant gradient optimization was used to minimize the total energy function. Convergence was considered to be achieved when the norm of the gradient of the energy was less than 0.10 kcal/mol, Å. All calculations on the precursor molecules **1** and **2** and radicals **1a** and **2a** in their respective crystal environments were performed on a VAX 8530 computer. In general computation took 2–3 hours of CPU time.

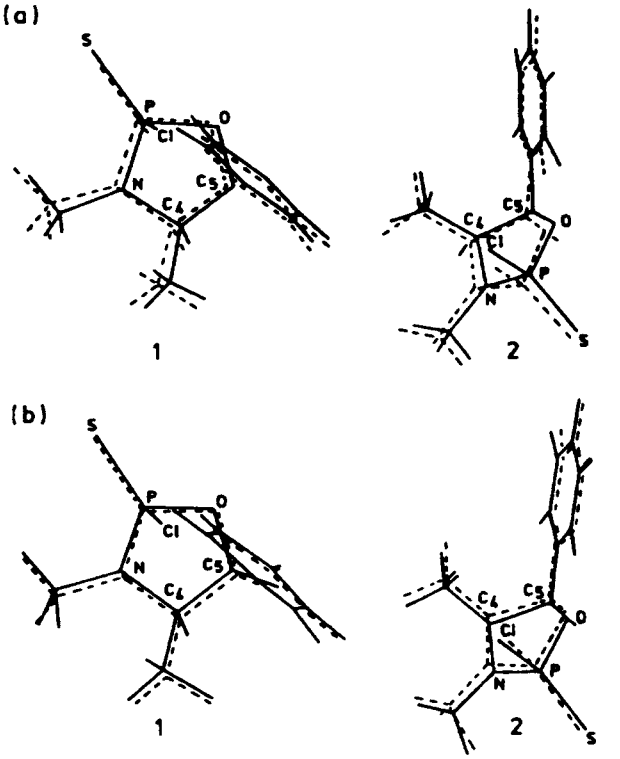

FIGURE 3 (a) Comparison of the initial crystal structure (straight line) with the optimized geometry of the radical precursor (dashed line) in compounds **1** and **2**.
(b) Comparison of the optimized radical structures **1a** and **2a** (straight line) with the optimized geometry of the parent precursor of **1** and **2** (dashed line).

RESULTS AND DISCUSSION

Conformational Feature

The optimized geometries of the molecules **1** and **2** do not differ much from their initial crystal structures. The root mean square (RMS) of the deviation of the five-membered ring atoms (O_1, P_2, N_3, C_4, and C_5) was 0.17 and 0.26 Å for compounds **1** and **2** respectively. This deviation is the result of a small shift of the phospholidine ring leaving the phenyl substituent fixed on its original position (see Figure 3a). The internal parameters of the optimized structures do not deviate from the initial crystal structures. Comparison of the optimized radical structure with the optimized parent radical precursor rendered even smaller deviations, RMS = 0.12 and 0.17 Å for compounds **1** and **2** respectively (see Figure 3b). It is to be noted that in compound **2** the formation of a phosphoranyl radical leads to the largest change of geometry.

The optimized geometries of both radicals **1a** and **2a** possess an elongated P⋯Cl σ^* bond length of 2.76 and 2.75 Å, respectively, and the SPCl bond angle becomes 115.8° and 115.7°. In both radical states a considerable elongation can be achieved, although the corresponding acquired steric interactions are larger in **2** than in **1** (vide infra). The SPCl bond angle is smaller than the equilibrium bond angle set in the force field (120°). Apparently the opening of the SPCl angle is unfavorable in the crystalline state. In Figure 4 the optimized geometries of both the radical structures **1a** and **2a** and their crystal surroundings are depicted.

Energetics Feature

The contributions of the various interaction types to the total energy are given in Table 1. The total energy of the optimized crystal structure **1** is higher than that of the optimized crystal structure **2**, in accordance with the stability difference of the two molecular crystals (**1**: mp 58°C, **2**: mp 130°C) [1]. As can be expected in the molecular crystals, the

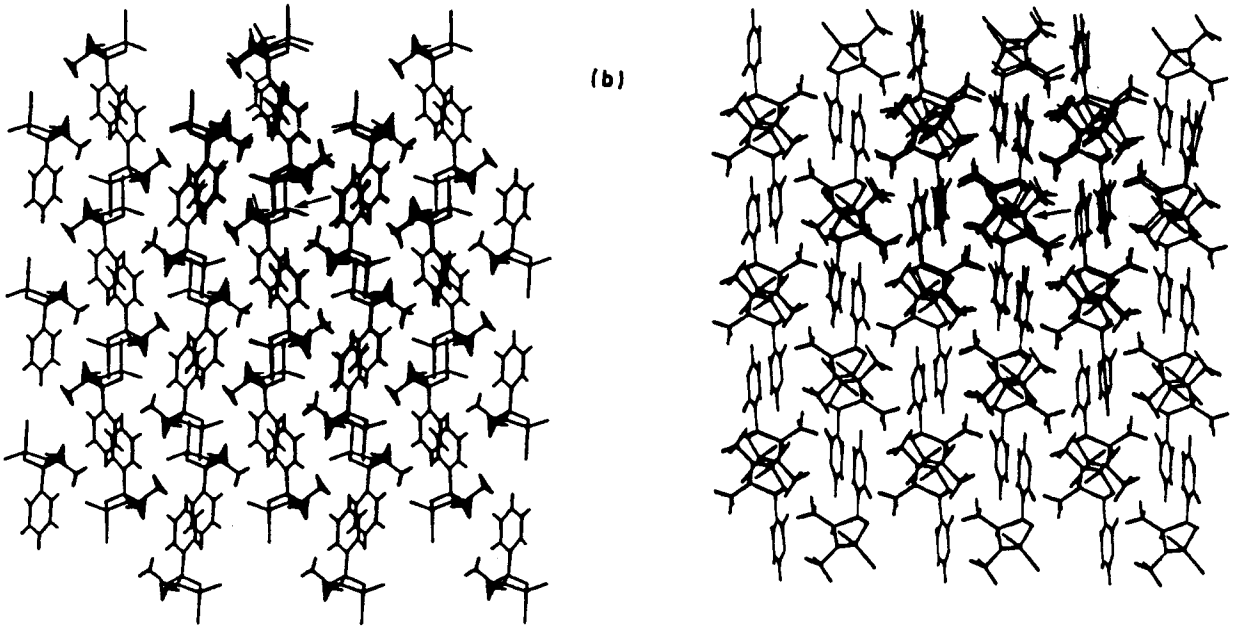

FIGURE 4 (a) Optimized geometry of radical **1a** and its crystal surroundings. An arrow indicates the radical location. (b) Optimized geometry of radical **2a** and its crystal surroundings. An arrow indicates the radical location.

Van der Waals energy gives the highest contribution to the total energy.

Mainly due to electrostatic interactions with the −1 charge distributed over the radical, the total energy of the radical **1a** and **2a** is lower than that of **1** and **2**, respectively. In Table 2 the differences in the total energies and their partitions to contributions from the various interaction types between radical state and precursor state are given. Table 2 reveals that the differences calculated are, in principle, of the same magnitude. However, the bond-bending energy and the Van der Waals interactions term are noticeably different, and the total stabilization of radical **1a** over **2a** (3.5 kcal/mol) is mainly

TABLE 1 Total Energies and Their Partitions to Contributions from Various Interaction Types in kcal/mol.

		E_{tot}[a]	E_{bond}[b]	E_{angle}[c]	$E_{dihedral}$[d]	E_{vdW}[e]	E_{elec}[f]	E_{14vdW}[g]	E_{14elec}[h]
I	**1**	−221.3	9.6	32.6	83.4	−300.8	−99.2	134.4	−81.3
II	**1a**	−241.1	9.6	31.2	84.3	−300.1	−111.4	134.6	−89.3
III	**2**	−282.6	6.7	36.4	70.6	−318.5	−101.3	123.5	−100.0
IV	**2a**	−298.9	7.0	36.7	71.1	−316.3	−113.3	123.6	−107.8

[a] E_{tot} is the total minimized energy.
[b] E_{bond} is the sum of all bond-stretching terms.
[c] E_{angle} is the sum of all bond-bending terms.
[d] $E_{dihedral}$ is the sum of all torsion contributions.
[e] E_{vdW} is the sum of all Van der Waals interactions.
[f] E_{elec} is the sum of all the electrostatic terms.
[g] E_{14vdW} is the sum of all Van der Waals interactions between atoms separated by only two other atoms.
[h] E_{14elec} is a similar sum for the electrostatic interactions.

TABLE 2 Differences in the Total Energies and Their Partitions to Contributions from Various Interaction Types between the Radical Structure and the Radical Precursor in kcal/mol (**1a** − **1** and **2a** − **2**)

		E_{tot}	E_{bond}	E_{angle}	$E_{dihedral}$	E_{vdW}	E_{elec}	E_{14vdW}	E_{14elec}
V	II − I	−19.8	0.0	−1.4	0.9	0.7	−12.2	0.2	−8.0
VI	IV − III	−16.3	0.3	0.3	0.5	2.2	−12.0	0.1	−7.8
VII	V − VI	−3.5	−0.3	−1.7	0.4	−1.5	−0.2	0.1	−0.2

constituted of these two. The larger Van der Waals interactions calculated in **2** are consistent with our previous work [1].

The increase in the Van der Waals energy is 0.7 kcal/mol for **1** and 2.2 kcal/mol for **2**. Considering this contribution to be important to the kinetics of the reaction: P—Cl + $e^- \xrightarrow{k}$ P·⁻Cl σ^* at 77 K ($k = k_0 \times \exp(-E_{vdw}/0.154)$, the Van der Waals interactions will slow down the reaction 94 times in **1** and 1.6×10^6 in **2**. Thus, steric interactions will decrease a phosphoranyl radical formation 1.7×10^4 times more in **2** than in **1**.

CONCLUSIONS

In this paper we present molecular mechanics calculations on the P·⁻Cl σ^* radical formation in compounds **1** and **2**. Our goal was to extend our previous modelling studies allowing the geometry of the radical precursor and its surroundings to adjust to the elongation of the P—Cl bond. The calculations do not exclude the formation of a long P—Cl bond in both compounds. However, they do show that occurrence of long P—Cl bonds in crystalline **1** and **2** will lead to higher Van der Waals interactions in compound **2** than in **1**. This is in qualitative agreement with the single-crystal experiments and Van der Waals calculations without geometry optimization reported previously [1].

The rate of stabilization of an initial electron-adduct toward a stable configuration determines the overall radiation process. Provided geometry relaxation is fast and will lead to sufficiently deep traps, the anion radical can be detected by ESR spectroscopy [12]. The interference of stabilization by steric interactions will favor a recombination reaction of the "free electron" with its parent radical cation or another electron-loss process. In the present case it appears that, in spite of Van der Waals interactions encountered in compound **1**, stabilization towards a P·⁻Cl σ^* configuration is possible, whereas in compound **2** this is not feasible due to the larger steric interactions. The calculated drop in reaction kinetics is in accordance with this assumption.

The theoretical description of radical formation is done by quantum chemical calculations. These studies strictly apply only to isolated systems. The extrapolation of such a calculated process in molecular crystals is not straightforward because the extra effect of intermolecular interactions has to be taken into account. At the present time a full quantum chemical description of radical formation in a surrounding crystal environment is not feasible. We have shown that molecular mechanics can give an adequate description of the steric interactions encountered upon radical formation. Unfortunately, molecular mechanics cannot give a complete description of the radical formation due to a poor representation of the radical structure. Therefore, we will extend our calculations by using a combination of both quantum chemical calculations and molecular mechanics to obtain a better insight into radical formation in molecular crystals. For this purpose, we will use the QUEST program [13] (part of the AMBER package). In this program, the total structure can be divided into a quantum chemical part (the radical) and a molecular mechanics or dynamics part (the crystal surroundings of the radical), and the optimization of the geometries of both parts is done simultaneously with mutual influence.

ACKNOWLEDGMENT

The investigation has been supported by the Netherlands Foundation for Chemical Research (SON) with financial aid from the Netherlands Organization for Scientific Research (NWO). We thank Mr. Henk Eding for assistance in the layout.

REFERENCES

[1] O. M. Aagaard, R. A. J. Janssen, B. F. M. de Waal, H. M. Buck, *J. Am. Chem. Soc., 112,* 1990, 938.

[2] (a) G. M. J. Schmidt, *Pure Appl. Chem., 27,* 1971, 647. (b) M. D. Cohen, *Angew. Chem., Int. Ed. Engl., 14,* 1975, 386. (c) J. R. Scheffer, J. Trotter, *Rev. Chem. Intermed., 9,* 1988, 271. (d) V. Ramamurthy, K. Venkatesan, *Chem. Rev., 87,* 1987, 433. (e) H. E. Zimmerman, M. J. Zuraw, *J. Am. Chem. Soc., 111,* 1989, 2358 and 7974.

[3] U. C. Singh, P. K. Weiner, J. W. Caldwell, P. A. Kollman, AMBER (UCSF version 3.0), Dept. Pharmaceutical Chemistry, University of California, San Francisco (1986).

[4] (a) for **1**: T. Bartczak, Z. Galdecki, M. Rutkowska, *Acta Crystallogr., C39,* 1983, 222. (b) for **2**: T. Bartczak, Z. Galdecki, *Acta Crystallogr., C39,* 1983, 219.

[5] AMPAC program, Quantum Chemistry Program Exchange No. 506.

[6] S. J. Weiner, P. A. Kollman, D. A. Case, U. C. Singh, C. Ghio, G. Alagona, S. Profeta Jr., P. Weiner, *J. Am. Chem. Soc., 106,* 1984, 765.

[7] S. J. Weiner, P. A. Kollman, D. T. Nguyen, D. A. Case, *J. Comput. Chem., 7,* 1986, 230.

[8] Lange's Handbook of Chemistry, J. A. Dean (ed), 12th ed., McGraw-Hill, New York, p. 3–126 (1979).

[9] (a) O. M. Aagaard, R. A. J. Janssen, B. F. M. de Waal, H. M. Buck, *J. Am. Chem. Soc., 112,* 1990, 5432. (b) N. L. Allinger, J.-H. Lii, *J. Comput. Chem., 8,* 1987, 1146, for sp^2 C and H. N. L. Allinger, Y. H. Yuh, MM2 program, QCPE 395, for sp^3 C, O, N, P and S.

[10] (a) R. A. J. Janssen, M. H. W. Sonnemans, H. M. Buck, *J. Chem. Phys., 84,* 1986, 3694. (b) R. A. J. Janssen, M. J. van der Woerd, O. M. Aagaard, H. M. Buck, *J. Am. Chem. Soc., 110,* 1988, 6001.

[11] (a) R. A. J. Janssen, M. H. W. Sonnemans, H. M. Buck, *J. Am. Chem. Soc., 108,* 1986, 6145. (b) A. Hasegawa, K. Ohnishi, K. Sogabe, M. Miura, *Mol. Phys., 30,* 1975, 1367. (c) J. M. Howell, K. F. Olsen, *J. Am. Chem. Soc., 98,* 1978, 7119.

[12] M. C. R. Symons, *Pure Appl. Chem., 53,* 1981, 223.

[13] QUEST program: U. C. Singh, P. A. Kollman, *J. Comput. Chem., 7,* 1986, 718.